

# Study of Effects of pH on the Stability of Domains in Myosin Rod by High-Resolution Differential Scanning Calorimetry†

Antonio Bertazzon and Tian Yow Tsong\*

Department of Biochemistry, University of Minnesota College of Biological Sciences, St. Paul, Minnesota 55108

Received January 8, 1990; Revised Manuscript Received April 2, 1990

**ABSTRACT:** Differential scanning calorimetry (DSC) has detected at least six quasi-independent structure domains in myosin rod [Potekhin, S. A., & Privalov, P. L. (1978) *Biofizika* 23, 219-223]. These domains were found to be remarkably sensitive to pH in the physiological range, i.e., pH 6-8. We compared the thermodynamic characteristics, and studied effects of pH on the stability, of individual domains in rod, light meromyosin (LMM), and subfragment 2 (S-2). In rod, the lowest stability domain (approximately 400 amino acid residues per double strand), with a  $T_m$  of 42.4 °C, a  $\Delta H_{cal}$  of 190 kcal/mol, and a  $\Delta G$  of 3.39 kcal/mol, at pH 7.02, destabilized by absorption of protons, is located at the LMM/S-2 junction and split into two parts, one associated with S-2 (approximately 100 residues per double strand) and the other with LMM (300 residues per double strand). The fragment with S-2 is likely a part of the "hinge" suggested by Swenson and Ritchie [(1980) *Biochemistry* 19, 5371-5375]. All other domains of rod released protons on melting. The domains located in S-2 were the most sensitive to pH and released a total of 0.9 proton on melting. The thermal meltings of all domains in myosin rod, LMM, and S-2 were independent of each other, and enthalpies of melting were additive in the whole pH range studied. Their sensitivities to pH and KCl were also unaffected by the presence or absence of other fragments. For example, domains in an isolated S-2 behaved similarly as they were in the rod, and so were domains in LMM. The three fragments studied here also exhibited nearly the same specific heat of unfolding, i.e.,  $4.24 \pm 0.30$  cal/g,  $4.18 \pm 0.35$  cal/g, and  $4.01 \pm 0.60$  cal/mol for rod, LMM, and S-2, respectively. At least two of the six domains ( $T_m$ 's of 44.6 and 46.2 °C at pH 7.02) in the rod showed less than full cooperativity in melting ( $\Delta H_{vH}/\Delta H_{cal} < 1$ ) at pH below 6.8. Deconvolution of these rod endotherms into more than six domains was attempted, but unique solutions were not attainable. However, the endotherms of LMM and S-2, at all pHs, could be fitted, respectively, into five and three two-state-like transitions. Thermodynamic parameters associated with each of these transitions were extracted and their meaning discussed. We have also found that the two most stable domains of the rod changed their relative sizes with pH, suggesting migration of structure from one domain to the other upon protonation of certain histidine residue(s).

Myosin is a dimer in solution, consisting of two globular heads, referred to as S-1, which are attached to the end of a long, double-coiled coil helix, rod. The rod is approximately 154 nm in length (Steward & Edwards, 1984) and 2 nm in width (Slayter & Lowey, 1967). Recent measurements with scanning tunneling microscopy (STM) show a minimum width of 1.3 nm and a maximum width of 1.9 nm (Bertazzon & Tsong, 1990a) for the rod from rabbit muscle. Although these studies do not reveal unusually nonuniform structural features in the rod, other physical methods are able to detect quasi-independent structural domains with varied thermal stabilities within the molecule (Burke et al., 1973; Goodno & Swenson, 1975a,b; Tsong et al., 1979, 1983; Stafford, 1985; King & Lehrer, 1989). The presence of domains of distinct thermal stabilities has been shown earlier using spectroscopic techniques (Burke et al., 1973). However, DSC is a particularly sensitive technique for resolving structural domains, and as many as six independent transitions have been determined for the rabbit myosin rod (Potekhin & Privalov, 1978; Potekhin et al., 1979). Other advantages of DSC include the ability to distinguish a two-state process from a non-two-state processes by comparing the calorimetric enthalpy with the calculated van't Hoff enthalpy, and the relative easiness for extracting thermodynamic parameters from a DSC endotherm.

The rod may be cleaved into two parts by trypsin, at high ionic strength (Lowey et al., 1969), releasing the carboxyl-

terminal fragment, or light meromyosin (LMM), and subfragment 2 (S-2), which is located between the LMM and the globular head. The stability of these two fragments is sensitive to variations in pH (Segall & Harrington, 1967; Goodno et al., 1976; Swenson & Ritchie, 1980). However, different domains within these fragments exhibit different sensitivities to pH. Therefore, by combining enzymatic cleavage with pH modulation in a systematic study, one should be able to obtain information on the thermal stability and pH regulation of size and structural characteristics of these domains. We report here a detailed study of the stability, energetics, and effects of pH on myosin and its subfragments using high-sensitivity differential microcalorimetry.

## MATERIALS AND METHODS

**Chemicals.** All chemicals, unless specified, were purchased from Sigma (St. Louis, MO) and were analytical grade. Trypsin was purchased from Worthington (Freehold, NJ), and bovine pancreas  $\alpha$ -chymotrypsin (type VII, TLCK treated) was from Sigma (St. Louis, MO). pH standards were purchased from Fisher Chemical Co. (Fair Lawn, NJ).

**Protein Purification.** Myosin was purified according to Segall and Harrington (1967), modified as previously described (Bertazzon & Tsong, 1989), from white New Zealand male rabbits. Only fast-twitching white muscles, i.e., paravertebral (latissimus dorsi), were used. Myosin was enzymatically digested to obtain subfragments. Rod was prepared as previously described (Bertazzon & Tsong, 1989). The purity of rod preparations ranged from 80 to 98%. One of the con-

† This work was supported by NIH Grant GM 37304.

taminants was LMM as indicated by its molecular weight and its characteristic DSC endotherm. Only preparations with greater than 95% purity or more were used for data acquisition; the others were further digested to prepare S-2.

LMM was prepared as described (Nyitrai et al., 1983) with no further modifications. S-2 was prepared from tryptic digestion of rod as described by Sutoh et al. (1978) with the following modification. The digestion mixture was collected by reducing the pH to 5.0, resuspended in 10 mM Tris-HCl, pH 7.0, including 0.1 M KCl, and centrifuged at 16 000 rpm for 20 min. Under these conditions, LMM and undigested rod were insoluble, and the supernatant contained S-2 of varying sizes (Sutoh et al., 1978). The two longer fragments were recovered by the addition of  $\text{CaCl}_2$  to the solution (final concentration of 5 mM). Further purification was achieved with HPLC ion-exchange chromatography using an LKB HPLC, equipped with an LKB 2150 pump, a mixing valve, an LKB 2152 controller, and an LKB 2151 UV-Vis monitor. The ion-exchange column used was an Ultropak TSK SWP ( $7.5 \times 75$  mm). Proteins were recovered by using an LKB Helirac 2212 fraction collector. Proteins, up to 20  $\mu\text{g}$ , were loaded onto the column after equilibration with 10 mM Tris-HCl, pH 6.5 (buffer A), and a linear step gradient was applied of increasing ionic strength from 0 to 0.3 M KCl (10 mM Tris-HCl, pH 6.5, and 0.3 M KCl, buffer B). The steps were 10 min from 0 to 20% buffer B, 10 min at 20% B, and 10 min from 20 to 100% B at a flow rate of 1 mL/min. Two peaks, one with molecular weight of 115K (dimer) and the other of 100K, appeared with retention times of 11 and 12 min, respectively. Both peaks were either studied separately or pooled together for experiments.

**Protein Concentration and Characterization.** Absorption coefficients ( $E_{280}^{1\%}$ ) of 3.5 (Weeds & Pope, 1977) for LMM, 2.1 for rod (Geoffrey & Harrington, 1970), and 0.7 for S-2 (Sutoh et al., 1983) were used to calculate protein concentration. The colorimetric method of Lowry et al. (1951) was also used with bovine serum albumin as a standard. Molecular size was determined with SDS-PAGE using the standard technique described by Laemmli (1970) with acrylamide concentrations of 4% and 10%, respectively, in a stacking and separating gel. The gel dimension was  $16 \times 16$  cm, and Bio-Rad high and low molecular weight standards were used. For routine purity checks, a Bio-Rad Mini Protean II system was used. Gels were scanned with a Zenith Soft Laser Model SL-504-XL scanning densitometer.

**Thermal Denaturation.** Differential scanning calorimetry (DSC) was done with a Microcal MC 2 microcalorimeter, interfaced to an AT&T PC 6300 personal computer through an A/D converter (Data Translation board DT2801) and a Hewlett Packard ColorPro plotter. Protein concentration ranged from 1.5 to 16 mg/mL, and the capacity of the cells was 1.241 mL. The reversibility of the thermal denaturation depended on the conditions used, but with the conditions of pH and/or ionic strength used in this study, reversibility varied between 80 and 95%. The absolute temperature reading of the instrument was calibrated by the company at 28 and 79  $^{\circ}\text{C}$ , using pure hydrocarbons. No dependence of the DSC endotherm was detected for heating rates ranging from 10 to 90  $^{\circ}\text{C}/\text{h}$ . Some early experiments were done using a Model MC-1 microcalorimeter (Microcal, Amherst, MA), and the data were digitized with a Summasketch digitizing tablet, were stored on disk using Sigmascan software, and were analyzed with a Cpfir program kindly provided by Dr. E. Freire.

**Calorimetric Data Analysis.** Data analysis was performed by using the software package provided by the Micro Cal

(EMF Software). The deconvolution program is based on the procedure described by Freire and Biltonen (1978a,b). The complex endotherm may be resolved into several transitions each defined by a melting temperature, a calorimetric  $\Delta H$ , and a van't Hoff  $\Delta H$ , using a least-squares fitting procedure. The calorimetric enthalpy of denaturation, defined in eq 1, is obtained directly by integrating the measured average excess heat capacity,  $\langle \Delta C_p \rangle$ :

$$\langle \Delta H \rangle = \int_{T_0}^T \langle \Delta C_p \rangle dT \quad (1)$$

The van't Hoff enthalpy is described by

$$\Delta H_{\text{vH}} = 4RT^2 C_p(\text{max}) / \Delta H_{\text{cal}} \quad (2)$$

In eq 2,  $C_p(\text{max})$  is the maximal  $C_p$  of the DSC excess heat capacity curve. The partition function  $Q$  is experimentally determined by

$$Q(T) = \exp \int_{T_0}^T (\langle \Delta H \rangle / RT^2) dT \quad (3)$$

Because all endotherms of rod were found to exhibit three discernible  $T_m$ 's in the pH range we studied, i.e., from 6.2 to 7.3, these  $T_m$ 's were used as the reference in the deconvolution of endotherms. The following parameters were considered: the  $\Delta H_{\text{cal}}$  which gives the size of the transition;  $T_m$  which locates the thermal stability of a domain;  $\Delta C_p$  which indicates the change in the heat capacity of the denatured state compared to the native state; and  $\Delta H_{\text{vH}}$  which indicates the range of temperature in which the transition occurs (i.e., width of the transition). The cooperativity ratio, defined by  $\Delta H_{\text{vH}} / \Delta H_{\text{cal}}$ , was either set to be unity or allowed to adjust during the regression.

The  $\Delta C_p$  for a complete endotherm was determined by linearly extrapolating the pretransition base line to the posttransition temperature range. The posttransition base line was assumed to be linear, and the difference in  $C_p$  values for the denatured and the native states was assigned to be  $\Delta C_p$ . When an endotherm was resolved into several transitions, the  $\Delta C_p$  apportioned to each transition was proportional to its contribution to the enthalpy of the whole transition. In our experiments it was found that  $\Delta C_p$  values for the rod, LMM, and S-2 were dependent on protein concentrations; their values decreased with increasing protein concentrations, while  $\Delta H_{\text{cal}}$  was insensitive to the protein concentration. The increase in  $\Delta C_p$  occurred at protein concentrations below 5  $\mu\text{M}$ . The reason for these effects was not clear. As the transition of the myosin rod was completely reversible, it is not likely that protein aggregation was the cause. Consequently, we have arbitrarily used the concentration at 15  $\mu\text{M}$  for comparison of the different subfragments. In the rod, the  $\Delta C_p$  of  $0.11 \pm 0.03$  cal/(g·K) was experimentally determined for protein concentration at 15  $\mu\text{M}$ . This value is to be compared with 0.16 cal/(g·K) for ribonuclease A and 0.14 cal/(g·K) for staphylococcal nuclease. In our presentations and deconvolution analyses (e.g., Figures 1, 3, 4, and 6),  $\Delta C_p$  of a transition was removed by drawing a straight line connecting the onset and the end point of the endotherm. This procedure would have no effect on interpretation.

The free energy of unfolding for each domain was calculated from the deconvoluted endotherm by

$$\Delta G = -RT \ln K \quad (4)$$

where the equilibrium constant  $K$  at a specified temperature was obtained as the ratio of the heat absorbed up to that temperature and the total heat absorbed for the transition.

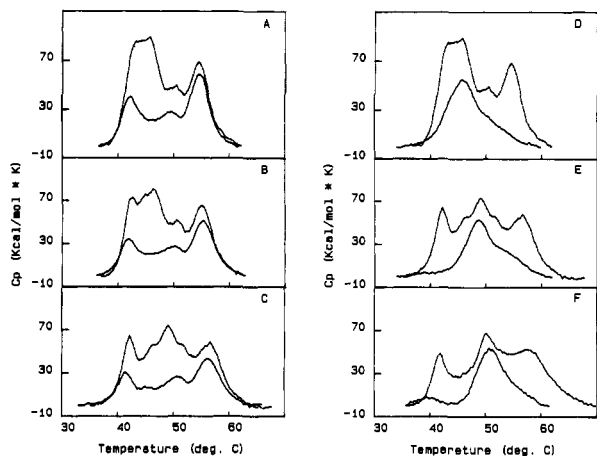


FIGURE 1: Effects of pH on the endotherms of myosin rod, LMM, and S-2. The buffer composition was 20 mM potassium phosphate, 0.5 M KCl, and 1 mM EDTA. The heating rate was 1 K/min. The protein concentrations were 4.2 mg/mL for the rod, 3.6 mg/mL for the LMM, and 2.3 mg/mL for the S-2. In panels A, B, and C, the molar enthalpy of the LMM (solid curves) is compared with that of the rod (dashed curves) at pH 7.02, 6.75, and 6.43, respectively. In panels D, E, and F, endotherms of S-2 (solid curves) and rod (dashed curves) are superimposed at pH 7.02, 6.43, and 6.2, respectively.

Equation 5 was then used to calculate the entropy of the transition:

$$\Delta S(T) = [\Delta H(T) - \Delta G(T)]/T \quad (5)$$

An alternative approach was to use eq 6:

$$\Delta G(T) = \Delta H(T) - T\Delta S(T) \quad (6)$$

in which  $\Delta H(T)$  was obtained from the calorimetric data as

$$\Delta H(T) = \Delta H(T_m) - \Delta C_p(T_m - T) \quad (7)$$

The entropy change was then calculated from the relationship

$$\Delta S(T) = \Delta H(T_m)/T_m - \Delta C_p \ln(T_m/T) \quad (8)$$

according to Privalov et al. (1986).

The number of protons associated with the thermal transition of S-2 was obtained as described elsewhere (Bertazzon et al., 1990).

## RESULTS

**Effect of pH on the Melting of Myosin Rod and Other Fragments.** The experimental endotherms for rod (solid curves in panels A–F), LMM (dashed curves in panels A–C), and S-2 (dashed curves in panels D–F), with varying pH, are shown in Figure 1. The endotherms for both the rod and the LMM were complex, and each could be grouped into three main peaks, with a different degree of sensitivity to the solution pH. The endotherms of S-2 were simpler in feature compared to that of the rod and the LMM, but they are highly asymmetrical, with broadening of the shape at the higher temperature end. The specific enthalpy for the rod,  $4.24 \pm 0.3$  cal/g, and for the LMM,  $4.18 \pm 0.35$  cal/g, was relatively constant throughout the pH range 8.0–6.1. At lower pH values, the protein aggregated with a reduction of the total enthalpy and the loss of the first transition (at pH 5.75). No enthalpy change was further detected at pH 5.2 where the protein was precipitated. Protein concentration, as well as heating rate, did not affect the specific enthalpy value. However,  $\Delta C_p$  was inversely related to protein concentration.

S-2 showed a qualitatively similar behavior. At higher pH values, the endotherm was sharper, and a small shoulder was observed at about 51 °C. As the pH decreased, the overall endotherm shifted toward the higher temperatures: the shoulder after the main peak became more pronounced, and

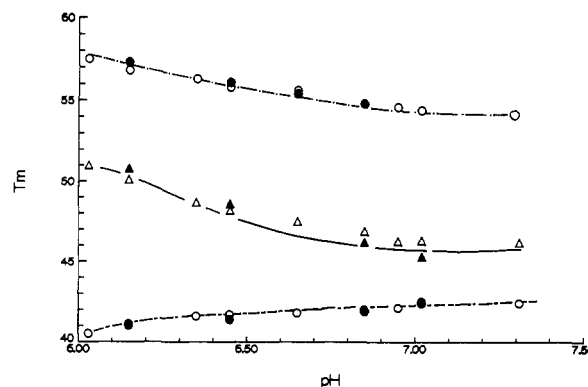


FIGURE 2: Comparison of the melting temperatures of the three major endotherm peaks of rod (open symbols) and the same peaks in the fragments (filled symbols). The peaks corresponding to LMM are represented with circles, and those of S-2 with triangles.

the main peak sharpened, again. A small endotherm also began to appear (panel F) and clearly detached at pH 6.2 (panel D). This endotherm was observed in the long S-2 by Swenson and Ritchie (1980) and was assigned to the melting of the "hinge". It would seem more likely, however, that the tryptic cleavage of the molecule results in splitting a domain into two parts. When the protein concentration was determined by UV absorption using a coefficient  $E_{280}^{1\%}$  of 0.7, the specific enthalpy calculated was  $3.24 \pm 0.6$  cal/g. When the protein concentration was determined by using a colorimetric assay (Lowry et al., 1951), the specific enthalpy was  $4.01 \pm 0.6$  cal/g. The specific enthalpies reported previously (Swenson & Ritchie, 1980), with the biuret method and UV absorption with the same coefficient, were  $3.2 \pm 0.6$  cal/g at pH 6.2 and  $2.2 \pm 0.4$  cal/g at pH 7.4. Variation of the specific enthalpy with the change in pH might arise from uncertainties in assigning proper base lines. However, in the later analysis, we will consider the specific enthalpy of S-2 to be similar to that of the other parts of the rod, i.e.,  $4.01 \pm 0.6$  cal/g. This choice made DSC data on all fragments self-consistent.

**Independence of Domains.** Different parts of the molecule reacted differently to a perturbation of the system (e.g., changing pH). The behavior of the  $T_m$ 's for the major peaks was similar in the whole rod as that in the LMM and S-2 fragments (Figure 2). The presence or absence of S-2 did not change the stability of domains belonging to LMM. Neither did the presence or absence of LMM change the stability of domains belonging to S-2. The buffer conditions were identical in these experiments, i.e., 20 mM  $KP_i$ , 0.5 M KCl, and 1 mM EDTA. At lower ionic strengths, S-2 showed a similar response to pH but with a larger shift of the  $T_m$ . For example, at pH 6.2, the  $T_m$  was 49 °C in 0.1 M KCl and was 39 °C in 0.5 M KCl.

The molar enthalpy calculated for a dimer of rod (252 kDa) was  $1068 \pm 75$  kcal/mol, and that of LMM (140 kDa) was  $585 \pm 49$  kcal/mol. The computer-calculated differential endotherm for S-2 is shown in Figure 3 (panel B) and was compared with the experimental curve (solid line), based on a specific enthalpy of  $4.01 \pm 0.6$  cal/g and a size of 120 kDa. The differential endotherm accounted for 460 kcal/mol which would give a molecular size of 115 kDa. The size and the enthalpy value are within experimental error. The differential endotherms obtained by subtracting S-2 from the rod were compared with experimental endotherms of LMM at the same pH in Figure 3 (panel A).

In agreement with Swenson and Ritchie (1980), we observed a small endotherm in S-2 which absorbed protons on melting. The transition was estimated to involve  $50 \pm 15$  kcal/mol.

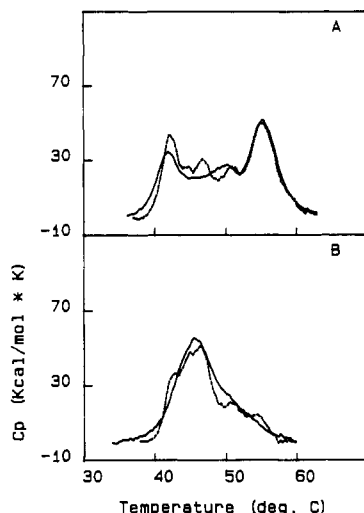


FIGURE 3: Computer-calculated differential endotherms. In panel A, the calculated difference between rod and S-2 (dotted line) is superimposed on the experimental endotherm obtained with LMM at pH 6.79 (solid line). In panel B, the difference between the endotherms of rod and LMM (dotted line) is compared with the experimental endotherm obtained with S-2 at pH 6.75.

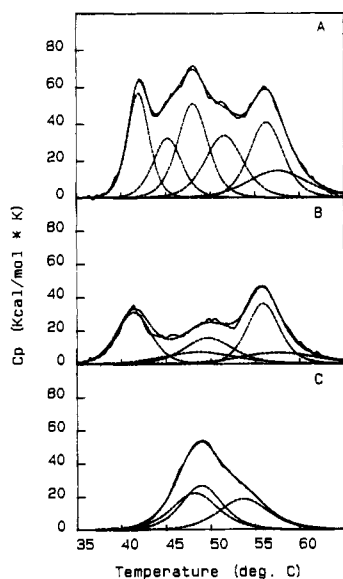


FIGURE 4: Deconvolution of endotherms of myosin rod, LMM, and S-2. In panel A, the excess heat capacity curve of myosin rod (pH 6.45) was resolved into six components. Solid lines represent the experimental curve, dotted lines are the fitting, and double-dashed lines are the individual components. Panels B and C show the deconvolution of LMM (pH 6.4) and S-2 (pH 6.5) endotherms, respectively. The transitions were two-state as defined by the cooperative ratio of unity. Numerical values are reported in Tables I, III, and IV.

Assuming a specific enthalpy of 4.2 cal/g, the molecular weight of this fragment would be about 12K, or a double strand of about 50 residues per strand. The difference in enthalpy in the first transition of the rod and LMM was  $40 \pm 7$  kcal/mol and was of a comparable size, suggesting that the domain was split during enzyme cleavage.

**Deconvolution of Endotherms.** The resolution of the endotherm into independent domains is shown in Figure 4. In panel A, the endotherm of the rod (pH 6.45) was resolved into six independent transitions, each defined by a melting temperature, a calorimetric enthalpy, and a van't Hoff enthalpy. The numerical values for the fitting are reported in Table I for different pHs. In general agreement with Potekhin and Privalov (1978), six was the minimal number of unique

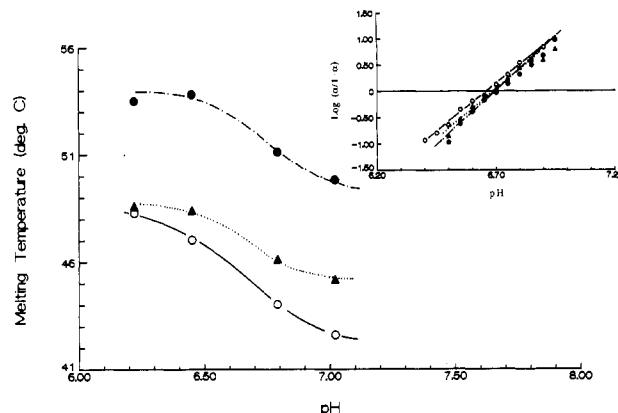


FIGURE 5: Melting temperatures, obtained from the deconvolution, of S-2 as a function of pH. From the slopes in the insert, the number of protons involved in the stability of S-2 were obtained.

transitions that would fit the endotherm at all the pHs considered. The first transition was, within experimental error, well described by a two-state process at all the pHs considered [in agreement with Privalov (1982)]. For the other transitions, the less than unit CR would suggest that the domain could be further resolved into subdomains. In Table II, the thermodynamic quantities obtained experimentally at different pHs are reported for the first transition in rod. The total enthalpy appeared to be constant ( $194 \pm 10$  kcal/mol). The van't Hoff enthalpy, given by the width of the transition, was also constant, with a value of  $209 \pm 5$  kcal/mol. Although the standard deviations of the calorimetric and van't Hoff enthalpies were small (i.e., 5% and 2.4%, respectively), it was not possible to obtain values of entropy accurately enough to interpret the enthalpic and entropic contributions to the change in stability determined by the pH. To overcome this limitation, a two-state transition, defined by an enthalpy of 210 kcal/mol with a  $T_m$  of 42.4 °C at pH 7.0 and a  $\Delta C_p$  of 4.5 kcal/(mol·K), was simulated. The thermodynamic quantities, calculated by using eq 6–8, at the observed melting temperatures are reported in Table II [columns specified by  $\Delta H(\text{th})$ ,  $\Delta S_{37}$ , and  $\Delta G_{37}$ ]. The transition showed a relatively large entropy [590 cal/(mol·K)], but the variation between pH 6.03 and pH 7.31 was very small,  $\Delta \Delta S = 4.1$  cal/(mol·K). The variation in enthalpy was also small,  $\Delta \Delta H = 8.5$  kcal/mol. However, it is more likely to be responsible for the reduction in stability at lower pH ( $\Delta \Delta G = 1.28$  kcal/mol). In the last column, the values were obtained through the equilibrium constant in experimental endotherms with a CR = 1.

Increasing the number of transitions in the deconvolution of rod endotherms did not provide additional information about the domains because the solution would not be unique. To overcome the problem, an independent fitting of S-2 and LMM was done, assuming each transition to be a two-state transition. The results for LMM and S-2 are reported in Tables II and III for different pH values. Five transitions gave the most reasonable fitting in LMM (Figure 4B), in agreement with Potekhin and Privalov (1979), over the pH range considered. For S-2, the best fit was three transitions (Figure 4C). Figure 5 reports the melting temperatures as a function of pH, calculated after deconvolution for S-2. As in the case of the thick filament [see Bertazzon and Tsong (1990b)], the melting temperature of S-2 transitions seems to be described as a sigmoidal function of pH. In the insert, the protons involved were estimated to be 0.3 proton per domain, with an inflection point at pH 6.7. This should be compared to 2.17 proton per mole (inflection point at pH 6.82) obtained with the thick filament in 0.1 M KCl.

Table I: Deconvolution of Endotherms of Myosin Rod<sup>a</sup>

	domain					
	I	II	III	IV	V	VI
pH 6.03						
$T_m$	40.5	46.0	51.0	53.0	55.5	57.5
$\Delta H_{cal}$	188	158	189	100	111	136
CR	1.1	0.7	0.9	1.2	1.1	1.1
pH 6.15						
$T_m$	41.1	45.5	50.1	52.6	56.8	56.9
$\Delta H_{cal}$	207	217	246	144	155	139
CR	1.0	0.7	0.7	1.0	1.0	1.0
pH 6.35						
$T_m$	41.6	45.6	48.7	52.0	56.7	56.9
$\Delta H_{cal}$	188	184	225	124	171	138
CR	1.1	0.7	0.8	1.0	0.7	0.9
pH 6.45						
$T_m$	41.7	45.4	48.2	51.6	56.2	56.3
$\Delta H_{cal}$	193	191	255	142	186	147
CR	1.12	0.8	0.7	1.0	0.6	0.9
pH 6.65						
$T_m$	41.8	45.1	47.5	50.8	55.7	55.8
$\Delta H_{cal}$	210	204	278	154	142	100
CR	1.0	0.7	0.6	0.6	1.2	0.9
pH 6.85						
$T_m$	41.9	45.2	46.9	50.5	55.4	55.9
$\Delta H_{cal}$	175	182	277	151	153	148
CR	1.25	0.8	0.6	0.7	1.2	0.6
pH 6.95						
$T_m$	42.1	44.7	46.3	50.5	54.8	55.1
$\Delta H_{cal}$	201	158	238	144	163	124
CR	1.0	1.0	0.8	1.0	1.2	0.6
pH 7.02						
$T_m$	42.4	44.7	46.3	50.4	54.6	55.1
$\Delta H_{cal}$	190	139	240	122	161	105
CR	1.1	1.0	0.8	1.0	1.2	1.2
pH 7.31						
$T_m$	42.4	44.6	46.2	50.2	54.4	54.8
$\Delta H_{cal}$	193	156	233	122	159	101
CR	1.1	1.1	0.9	1.2	1.2	0.5

<sup>a</sup>  $T_m$  is given in degrees centigrade,  $\Delta H_{cal}$  in kilocalories per mole, and the cooperative ratio (CR) defined as  $\Delta H_{vH}/\Delta H_{cal}$ . Solvent compositions were 20 mM potassium phosphate, 0.5 M KCl, and 1 mM EDTA. The uncertainty in  $\Delta H_{cal}$  for the rod was 6% (>10 determinations) and for each domain was 10% (>10 determinations). The uncertainty for  $\Delta H_{vH}$  was 5% for the rod and for each domain was also 5%, each with greater than 10 determinations.

Table II: Effect of pH on the Enthalpic and Entropic Contributions to the Stability of Transition I in Myosin Rod<sup>a</sup>

pH	$T_m$	$\Delta H_{cal}$	$\Delta H_{vH}$	$\Delta H(th)$	$\Delta S_{37}$	$\Delta G_{37}$	$\Delta G_{37}(I)$
6.03	40.5	188	206	201	592	2.1	
6.15	41.1	207	207	204	591	2.5	2.53
6.35	41.6	188	206	206	580	2.9	
6.45	41.7	193	216	207	589	3.0	
6.65	41.8	210	210	207	589	3.0	3.13
6.85	41.9	175	218	208	589	3.0	
6.95	42.1	201	201	208	589	3.1	3.07
7.02	42.4	190	209	210	588	3.4	
7.31	42.4	193	210	210	588	3.4	3.33

<sup>a</sup> Enthalpy and free energy values are given in kilocalories per mole entropy in and calories per mole per degree kelvin. Melting temperatures are expressed in degrees centigrade. The reference enthalpy for calculating  $\Delta H(th)$  was 210 kcal/mol, the melting temperature was 42.4 °C, and the  $\Delta C_p$  was 4.5 kcal/(mol·K); each value was calculated for the observed melting temperature. See text for explanation.  $\Delta G_{37}(I)$  was calculated from eq 4, and the equilibrium constant was obtained as described under Materials and Methods. The uncertainty for  $\Delta H_{cal}$  was 5% and for  $\Delta H_{vH}$  was 2.4% (>10 determinations).

$\Delta C_p$  values obtained for 15  $\mu$ M solutions at pH 7.0 (3.8 mg/mL for rod, 2.1 mg/mL for LMM, and 1.73 mg/mL for S-2) were  $11 \pm 4$  kcal/mol for S-2,  $14 \pm 3$  kcal/mol for LMM, and  $27 \pm 5$  kcal/mol for rod: this corresponded to an average specific heat capacity of  $0.1 \pm 0.02$  cal/(g·K).

Two different thermodynamic approaches were used in the analysis. When the equilibrium constant of the transition obtained through the enthalpy change was used, the Gibbs free energy thus calculated did not depend on entropy and on  $\Delta C_p$  (eq 4). Conversely, the  $\Delta G$  can be calculated from eq 6 and enthalpy and entropy directly measured from the calorimetric curve (eq 7 and 8). Agreement between the two approaches

would be indicative of the reliability of the deconvolution procedure.

In Figure 6A–C, the third major peak in the endotherm of LMM is compared at different pHs. The peak was well-defined in the experimental endotherm and could be described by two transitions. However, the size, i.e., the enthalpy of the transition, varied greatly with changes in pH. The sum of the enthalpy of the two transitions was relatively constant ( $\Delta H_{cal}$  at pH 7.02 was 264 kcal/mol, panel A; at pH 6.5, 262 kcal/mol, panel B; and at pH 6.2, 233 kcal/mol, panel C). However, a continuous broadening of the peak indicative of a reduction of the van't Hoff enthalpy was observed ( $\Delta H_{vH}$

Table III: Deconvolution of the Endotherm of LMM<sup>a</sup>

pH	<i>T<sub>m</sub></i> (°C)	$\Delta H_{\text{cal}}$ (kcal/mol)	$\Delta C_p$ [kcal/(mol·K)]	$\Delta G_{37}$ (kcal/mol)		$\Delta S_{37}$ [cal/(mol·K)]	
				I <sup>b</sup>	II <sup>c</sup>	I <sup>b</sup>	II <sup>d</sup>
6.23	41.0	140	3.3	1.9	1.8	445	402
	47.0	101	2.4	2.9	4.9	316	245
	50.7	115	2.7	4.3	4.3	357	238
	56.3	100	2.4	4.8	4.4	158	307
	57.6	133	3.2	6.9	6.3	407	194
6.40	41.4	157	3.6	2.0	1.8	499	448
	48.7	78	1.8	2.5	2.6	108	243
	49.8	114	2.6	3.9	4.1	249	355
	55.9	177	4.1	8.9	7.5	291	542
	57.6	77	1.8	4.2	3.7	116	235
6.75	42.0	153	3.5	2.3	2.9	431	486
	48.2	72	1.7	2.2	2.2	164	225
	49.2	117	2.7	3.9	3.7	258	365
	55.4	182	4.2	9.5	8.3	308	556
	55.6	84	1.9	3.7	4.1	146	259
7.03	42.4	165	3.8	2.7	2.3	455	523
	48.8	70	1.6	2.2	2.0	157	219
	49.0	112	2.6	3.6	3.8	250	350
	53.7	63	1.5	2.8	2.7	114	194
	54.8	203	4.7	10.0	8.3	352	622

<sup>a</sup> Thermodynamic parameters were calculated as described under Materials and Methods. In the deconvolution, each domain was considered a two-state process (i.e.,  $\Delta H_{\text{cal}} = \Delta H_{\text{vH}}$ ). The uncertainty for  $\Delta H_{\text{cal}}$  was 8% (three to five determinations). The uncertainty in deconvolution was 5%.

<sup>b</sup> Obtained from eq 4. <sup>c</sup> Calculated from eq 6. <sup>d</sup> Calculated from eq 8.

Table IV: Deconvolution of the Endotherm of S-2<sup>a</sup>

pH	<i>T<sub>m</sub></i> (°C)	$\Delta H_{\text{cal}}$ (kcal/mol)	$\Delta C_p$ [kcal/(mol·K)]	$\Delta G_{37}$ (kcal/mol)		$\Delta S_{37}$ [cal/(mol·K)]	
				I <sup>b</sup>	II <sup>c</sup>	I <sup>b</sup>	II <sup>d</sup>
6.23	48.3	120	2.9	3.8	3.8	269	374
	48.7	144	3.5	5.0	4.7	317	448
	53.5	123	3.0	5.7	4.7	222	378
6.45	47.0	143	3.5	4.1	4.1	335	447
	48.4	145	3.6	4.9	4.4	321	451
	53.8	114	2.8	5.5	5.0	200	350
6.79	44.0	122	3.0	2.9	2.7	317	384
	46.1	154	3.7	4.0	4.0	375	484
	51.1	112	2.7	4.3	4.2	225	347
7.02	42.1	104	2.6	1.9	1.7	287	331
	44.7	158	3.9	3.6	3.6	401	497
	49.8	102	2.5	3.6	3.4	215	317

<sup>a</sup> Thermodynamic parameters were obtained as described under Materials and Methods. The deconvolution was done assuming a two-state process for each transition, and the fitting is shown in Figure 4. The uncertainty in  $\Delta H_{\text{cal}}$  and  $\Delta C_p$  was 20% (two to three determinations). This large uncertainty was due to the broadness of the endotherms which made the assignment of base lines difficult. <sup>b</sup> Calculated according to eq 4.

<sup>c</sup> Calculated according to eq 6. <sup>d</sup> Calculated according to eq 8.

was 171, 153, and 116 kcal/mol, respectively).

## DISCUSSION

The specific enthalpies obtained for rod ( $4.24 \pm 0.3$  cal/g) and LMM ( $4.18 \pm 0.35$  cal/g) were slightly less than that reported by Potekhin and Privalov (1978) of 4.6 cal/g. S-2 had a similar specific enthalpy of  $4.01 \pm 0.60$  cal/g when the concentration was determined by the Lowry method.

The cleavage of myosin with trypsin split the domain with the lower melting temperature in rod into two fragments. The domain was characterized by a  $\Delta H$  of  $194 \pm 10$  kcal/mol, which corresponds to a size of 200 residues per strand if we consider the specific enthalpy to have a constant value of 4.2 cal/g. The same domain in LMM was characterized by an average  $\Delta H$  of  $154 \pm 10$  kcal/mol, corresponding to 158 residues per strand. The small domain that clearly appeared in S-2 at low pH, previously identified by Swenson and Ritchie (1980), which responded to a pH analogous to that of the domain in LMM, showed a  $\Delta H$  of about 40 kcal/mol. Assuming a specific enthalpy of 4.1 cal/g, it corresponded to a domain of approximately 50 residues per strand. The previous estimate (Swenson & Ritchie, 1980) gave a size of about  $30 \pm 15$  kcal/mol and about 30–40 residues per strand, which is compatible with the present estimate. This low-stability

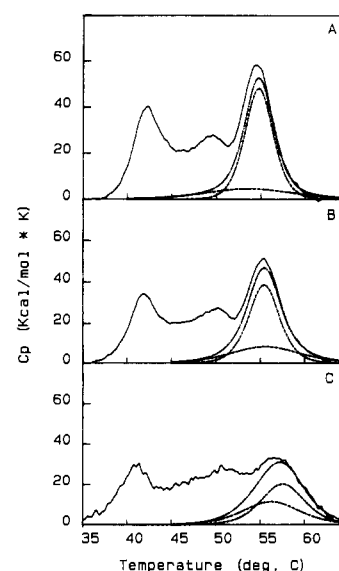


FIGURE 6: Last two domains obtained from the deconvolution of LMM (double dashed line) are combined (dotted line) and compared with the experimental endotherm (solid line) at pH 7.02 (panel A), 6.50 (panel B), and 6.29 (panel C). Numerical values are given in Table III.

fragment was assigned by Privalov (1982) to the region of LMM adjacent to S-2, suggesting that this was not an enthalpy of unzipping of the coiled coil. The conclusion that it was split into two parts, the bigger one belonging to LMM and the smaller one to S-2, reinforces the assignment of the domain to the region proposed and the concept that the double-coiled structure melts as a single cooperative unit. The transition in myosin rod was well-defined experimentally. This allows an estimate of the contributions of enthalpy and entropy to the stability of the domain. The analysis of the simulated process (Table II) shows that the domain is characterized by a relatively high entropy [590 cal/(mol·K)] and that a  $\Delta\Delta S$  of 4.1 cal/(mol·K) is insignificant compared to the total value of  $\Delta S$ . It is likely that the stabilization of 1.28 kcal/mol ( $\Delta\Delta G$ ) at higher pH of the domain is due to the effect of pH on enthalpy (although the  $\Delta\Delta H$  is also relatively small, i.e., 8.5 kcal/mol). This is the only well-defined domain which was destabilized by a pH reduction.

In the preceding paper (Bertazzon & Tsong 1990b), it was shown that at low ionic strength (0.1 M KCl) a part of the helix in myosin, conceivably S-2, was responsible for its sensitivity to pH, and reported the number of protons involved to be 2.17 per mole. In solution at higher ionic strength, i.e., 0.5 M KCl, each of the transitions seemed to contribute to a total of 0.9 proton per mole. The inflection point was at pH 6.82 in the filaments and at pH 6.7 in this study. A release of protons upon melting was reported earlier by Goodno and Swenson (1975a,b), Swenson and Ritchie (1980), and Tsong et al. (1979).

The set of transitions corresponding to the most stable part of the molecule has been assigned to the carboxyl terminal of the helical tail (Potekhin & Privalov, 1978; Privalov, 1982). Some discrepancies can be observed with the endotherms reported by Potekhin and Privalov (1978) for the tryptic fragment. A longer incubation with trypsin resulted in a reduction of this group of transitions, which seems ascribable to the removal of the carboxyl-terminal fragment (Niytrai et al., 1983). Comparison with the endotherm of the rod obtained with chymotrypsin digestion of the thick filament, and the short reaction time with trypsin, indicates that the endotherm was not missing this fragment. It is interesting to notice that the sum of the two domains is relatively well-defined, with a relatively stable size (260 kcal/mol), but clearly broadens at lower pH values. Two two-state domains can be fit into the transition. The contribution of each of them showed a change in enthalpy (Figure 6, Table III). This could be interpreted in terms of strong changes in the specific enthalpy of a well-defined group of residues, or a change in the size of the domain; i.e., electrostatic forces might be the reason for the definition of the domains.

The free energies calculated at 37 °C for the different domains increased for S-2 as the pH decreased. For LMM, both the most unstable and the most stable domains showed a decrease in free energy with decreasing pH, whereas free energies of other domains increased.

#### ACKNOWLEDGMENTS

We thank C. J. Gross for help with the manuscript.

#### REFERENCES

- Bertazzon, A., & Tsong, T. Y. (1989a) *Fed. Proc., Fed. Am. Soc. Exp. Biol.* 46, 2129.
- Bertazzon, A., & Tsong, T. Y. (1989b) *Biochemistry* 28, 9784-9790.
- Bertazzon, A., & Tsong, T. Y. (1990a) *Biophys. J.* 57, 333a.
- Bertazzon, A., & Tsong, T. Y. (1990b) *Biochemistry* (preceding paper in this issue).
- Bertazzon, A., Tian, G. H., Lamblin, A. F., & Tsong, T. Y. (1990) *Biochemistry* 29, 291-298.
- Burke, M., Himmelfarb, S., & Harrington, W. F. (1973) *Biochemistry* 12, 701-710.
- Freire, E. M. (1989) *Comments Mol. Cell. Biophys.* 6, 123-140.
- Freire, E. M., & Biltonen, R. L. (1978a) *Biopolymers* 17, 463-479.
- Freire, E. M., & Biltonen, R. L. (1978b) *Biopolymers* 17, 481-496.
- Geoffrey, J. E., & Harrington, W. F. (1970) *Biochemistry* 9, 886-893.
- Goodno, C. C., & Swenson, C. A. (1975a) *Biochemistry* 14, 867-872.
- Goodno, C. C., & Swenson, C. A. (1975b) *Biochemistry* 14, 873-878.
- Goodno, C. C., Harris, T. A., & Swenson, C. A. (1976) *Biochemistry* 15, 5157-5160.
- King, L., & Lehrer, S. S. (1989) *Biochemistry* 28, 3498-3502.
- Laemmli, U. K. (1970) *Nature (London)* 227, 680-685.
- Lowey, S., Slayter, H. S., Weeds, A. G., & Baker, H. (1969) *J. Mol. Biol.* 42, 1-29.
- Lowry, O. H., Rosenbrough, N. J., Farr, A. L., & Randall, R. J. (1951) *J. Biol. Chem.* 193, 265-275.
- Niytrai, L., Mocz, G., Szilagy, L., Balint, M., Chen Lu, R., Wong, A., & Gergely, J. (1983) *J. Biol. Chem.* 258, 13213-13220.
- Potekhin, S. A., & Privalov, P. L. (1978) *Biofizika* 23, 219-223.
- Potekhin, S. A., Trapkov, V. A., & Privalov, P. L. (1979) *Biophysics (Engl. Transl.)* 24, 46-50.
- Privalov, P. L. (1982) *Adv. Protein Chem.* 35, 1-104.
- Privalov, P. L., Griko, Yu. V., & Venyaminov, S. Yu. (1986) *J. Mol. Biol.* 190, 487-498.
- Segall, D. L., & Harrington, W. F. (1967) *Biochemistry* 6, 768-787.
- Slayter, H. S., & Lowey, S. (1967) *Proc. Natl. Acad. Sci. U.S.A.* 58, 1611-1618.
- Stafford, W. F. (1985) *Biochemistry* 24, 3314-3321.
- Steward, M., & Edwards, P. (1984) *FEBS Lett.* 168, 75-78.
- Sutoh, K., Sutoh, K., Karr, T., & Harrington, W. F. (1978) *J. Mol. Biol.* 126, 1-22.
- Swenson, C. A., & Ritchie, P. A. (1980) *Biochemistry* 19, 5371-5375.
- Tsong, T. Y., Karr, T., & Harrington, W. F. (1979) *Proc. Natl. Acad. Sci. U.S.A.* 76, 1109-1113.
- Tsong, T. Y., Himmelfarb, S., & Harrington, W. F. (1983) *J. Mol. Biol.* 164, 431-450.
- Weeds, A. C., & Pope, B. (1977) *J. Mol. Biol.* 111, 129-157.